Generalized Line Loss Relaxation in Polar Voltage Coordinates

Jonathon A. Martin, *Student Member, IEEE*   Ian A. Hiskens, *Fellow, IEEE*

Abstract—It is common for power system behavior to be expressed in terms of polar voltage coordinates. When applied in optimization settings, loss formulations in polar voltage coordinates typically assume that voltage magnitudes are fixed. In reality, voltage magnitudes vary and may have an appreciable effect on losses. This paper proposes a systematic approach to incorporating the effects of voltage magnitude changes into a linear relaxation of the losses on a transmission line. This approach affords greater accuracy when describing losses around a base voltage condition as compared to previous linear and piecewise linear methods. It also better captures the true behavior of losses at conditions away from the flat voltage profile.

Index Terms—Piecewise-linear loss models; polar voltage representation.

I. Introduction

CALCULATION of power system losses is a basic requirement of many optimal power flow and power system control formulations. However, the nonlinear nature of losses is often difficult to capture within the modelling restrictions imposed by the problem structure. Early loss formulations considered system-wide losses, and directly related total losses to power injections through constant network parameters. This became known as the B-coefficient method [1]–[3]. A subsequent method relating system-wide losses to power injections was described in terms of network impedances and voltage angles [4]. Since that time, various methods have been proposed which expand upon those early formulations and describe total losses in terms of power injections using linear [5]–[7] and quadratic [8], [9] formulations.

Alternatively, losses may be computed on a line-by-line basis. This paper considers such formulations, where the losses on each line are expressed in terms of its end-bus voltages. The coordinate system used to describe network voltages determines the properties of such loss models. In rectangular voltage coordinates, the losses on a transmission line are given by a quadratic function and can be described using a cone constraint [10]. In polar voltage coordinates, transmission line losses are quadratic in terms of voltage magnitudes but include a cosine term capturing the effect of the angle difference across the line. Since voltage magnitudes typically remain close to 1 pu during normal operation, methods describing losses as a quadratic in the angle difference have gained popularity over recent years. Depending on the problem formulation this behavior can be represented using conic [11], [12] or

piecewise-linear [13], [14] constraints. The piecewise-linear approximation given in [15] similarly assumes that voltage magnitudes are close to unity to approximate current flow with active power flow. The squared power flow is then used to compute active power losses on a line.

The assumption that voltage magnitudes remain at 1 pu is convenient when detailed voltage information is not available. For example, this may be the only option if a linear dc power flow formulation is used. However, in situations where voltage magnitudes are available, including their effects on losses will improve the accuracy of the loss calculation. Under heavy loading conditions or in weak sections of a network, voltage magnitudes may vary significantly. In such cases, inclusion of voltage magnitude effects becomes vital. First-order [16] or second-order [17] Taylor-series expansions are commonly used to express the loss behavior in this higher dimensional space. Unfortunately, first-order approximations suffer large errors, as discussed in [17], since they do not capture the nonlinearity of the loss function and second-order approximations require quadratic representations.

This paper develops a relaxation method which captures the nonlinearity of transmission line losses when voltages are expressed in polar coordinates. It will be shown that an appropriately chosen set of linear inequality constraints can provide a convex relaxation that (locally) achieves an accurate description of transmission line losses. Given the nonconvexity of losses when voltages are expressed in polar form, care must be taken when formulating the linear inequality constraints so that accuracy is preserved.

The paper is organized as follows. Section II describes the requirements of the proposed loss formulation. Section III discusses the necessary characteristics of an accurate linear relaxation. Convexity of the loss function is considered in Section IV and a linear relaxation is presented. Section V discusses trends in the eigendecomposition of the loss function Hessian, while Section VI describes special cases when voltage magnitudes are fixed. Section VII compares the performance of the proposed method to the present state-of-the-art linear relaxation methods. Section VIII concludes the paper.

II. Formulation requirements

The proposed loss modelling approach is motivated by applications where the following requirements must be satisfied:

1) applicable within a linear constraint environment,
2) voltages are expressed in polar form (magnitudes and angles),
3) tight around a given base voltage condition,
4) describe losses for a specific line.

None of the loss modelling approaches listed in Section I meet this specification except the first-order Taylor-series expansion, but it fails to adequately capture the nonlinear behavior of the loss equation.

Since transmission line losses are nonlinear in terms of voltage magnitudes and angles, the first requirement necessitates the use of a relaxation underbounding the true nonlinear relationship. This condition also eliminates the use of quadratic constraint formulations. The second requirement excludes methods which only account for voltage angle differences but ignore the effects of voltage magnitude changes. The third requirement assumes the availability of a base voltage profile. The fourth requirement rules out methods that only compute total system losses.

The approach developed in Section IV meets all four requirements and affords greater accuracy than a simple linearization. Given base voltages (in polar coordinates) for the end buses of a transmission line, the first step is to linearize the loss equation at that voltage condition. The second step is to choose several nearby sets of end-bus voltages and linearize the loss equation at each of those additional voltage conditions. Each of the linearizations is relaxed into an inequality constraint and together they provide an underbound for the loss function. The process for selecting the additional sets of voltages is discussed in the following sections.

III. FORMING A SET OF LINEAR RELAXATIONS

The main objective in forming a relaxation using a set of linear inequalities is to approximate a nonlinear constraint while using a linear solver. The linear approximation must provide a balance between simplicity and accuracy.

A. Simplicity

Every constraint added to a set of linear inequalities increases the associated computation. Building a large set of linear inequalities to approximate a nonlinear function may achieve high accuracy but will increase solution time. The improvement in accuracy may not justify the increased computational complexity. Fewer constraints which are well selected may achieve similar accuracy while maintaining simplicity. Furthermore, linear inequality constraints that are not located in a relevant region of the solution space, and so are never binding, should be avoided. They add to the computational cost but contribute nothing to solution quality.

B. Tightness

Consider a set of linear inequalities that is obtained by linearizing a nonlinear function at a number of points. Each linear constraint provides the most accurate estimate of the nonlinear function around its linearization point, and therefore should be binding in the vicinity of that point. For example, assume that linear inequalities are generated at the points, $x_i, \; i = 1, ..., n$, and form an approximation which seeks to underbound a nonlinear function f. The resulting piecewise linear approximation of f returns the value,

$$f^{app}(x) = \max_{i \in \{1,...,n\}} \left\{ f(x_i) + \frac{\partial f}{\partial x}(x_i)(x - x_i) \right\}. \quad (1)$$
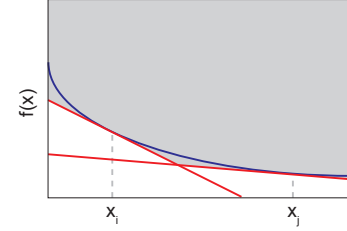
(a) Linear relaxation of a convex function.
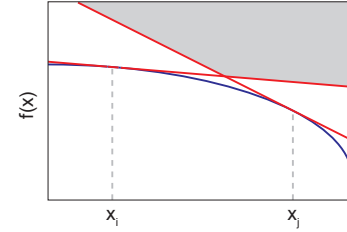
(b) Linear relaxation of a concave function.

Fig. 1. A set of linear inequality relaxations underbounds a convex function but not a concave function.

If the i-th constraint is binding then at the point x_i, (1) becomes $f^{app}(x_i) = f(x_i)$ which describes the best possible underbound of the true nonlinear function. This situation is illustrated in Fig. 1a. However, if the linearization around the point x_i is not the binding constraint then,

$$f^{app}(x_i) = f(x_j) + \frac{\partial f}{\partial x}(x_j)(x_i - x_j) > f(x_i), \quad (2)$$

for some $j \neq i$. This can occur if the function is nonconvex between x_i and x_j, with Fig. 1b providing an illustration. Examining the second-order Taylor-series expansion around x_j with $\Delta x = x_i - x_j$ offers further insight,

$$f(x_i) = f(x_j) + \frac{\partial f}{\partial x}(x_j)\Delta x + \tfrac{1}{2}\Delta x^{\mathsf{T}} \frac{\partial^2 f}{\partial x^2}(x_j)\Delta x + \text{h.o.t. (3)}$$

The error in the approximation, $f^{app}(x_i) - f(x_i) > 0$, will occur when,

$$\tfrac{1}{2}\Delta x^{\mathsf{T}} \frac{\partial^2 f}{\partial x^2}(x_j)\Delta x + \text{h.o.t.} < 0. \quad (4)$$

Assuming that the higher order terms are negligible, the error will be present when the second-order term in the Taylor-series expansion around x_j is negative along the path between x_i and x_j, implying concavity of f between x_i and x_j. If the function is convex on this interval then the error will not be present and the linearization at x_i will be tight.

The loss function is convex in some directions and concave in others when expressed in polar voltage coordinates. The next section quantifies this claim and discusses the handling of this nonuniform behavior when building a set of linear inequalities.

IV. CONVEXITY OF THE LOSS EQUATION IN POLAR VOLTAGE COORDINATES

A. Eigenstructure of the Hessian

In polar voltage coordinates, the function describing losses on a transmission line is an application of the law of cosines,

$$P_{ij}^{loss} = g_{ij}|V_i - V_j|^2$$
$$= g_{ij}\left(U_i^2 + U_j^2 - 2U_iU_j\cos(\delta_{ij})\right), \quad (5)$$

where P_{ij}^{loss} is the active power loss on line i–j, g_{ij} is the series conductance of the line, $V_i = U_ie^{\mathbf{j}\delta_i}$ and $V_j = U_je^{\mathbf{j}\delta_j}$ are the complex voltages at either end of the line, and $\delta_{ij} = \delta_i - \delta_j$ is the angle difference across the line.

To gain a better understanding of the behavior of the loss function expressed in (5), a second-order Taylor-series expansion can be formed by ignoring the higher-order terms in (3),

$$P_{ij}^{loss}(x + \Delta x) \approx P_{ij}^{loss}(x) + \nabla_x P_{ij}^{loss}(x)^\intercal \Delta x$$
$$+ \Delta x^\intercal \frac{\nabla_{xx}^2 P_{ij}^{loss}(x)}{2}\Delta x, \quad (6)$$

where $x \equiv [U_i \ U_j \ \delta_{ij}]^\intercal$. The gradient is given by,

$$\nabla_x P_{ij}^{loss}(x) = 2g_{ij}\begin{bmatrix} U_i - U_j\cos(\delta_{ij}) \\ U_j - U_i\cos(\delta_{ij}) \\ U_iU_j\sin(\delta_{ij}) \end{bmatrix}, \quad (7)$$

and the Hessian by,

$$\nabla_{xx}^2 P_{ij}^{loss}(x) = 2g_{ij}\begin{bmatrix} 1 & -\cos(\delta_{ij}) & U_j\sin(\delta_{ij}) \\ -\cos(\delta_{ij}) & 1 & U_i\sin(\delta_{ij}) \\ U_j\sin(\delta_{ij}) & U_i\sin(\delta_{ij}) & U_iU_j\cos(\delta_{ij}) \end{bmatrix}. \quad (8)$$

Example: For an operating condition with voltage magnitudes fixed at 1 pu and a small angle difference of 0.05 rad the gradient is given by,

$$\nabla_x P_{ij}^{loss}\left(\begin{bmatrix} 1 \\ 1 \\ 0.05 \end{bmatrix}\right) = 2g_{ij}\begin{bmatrix} 0.00125 \\ 0.00125 \\ 0.04998 \end{bmatrix}. \quad (9)$$

This supports the common hypothesis that voltage magnitudes have limited effect on the loss function since their sensitivities are close to zero. In contrast, the sensitivity of losses to angle difference is about 50 times larger.

If the operating condition deviates slightly, however, the effects of voltage magnitudes become more pronounced. Consider the case with $U_i = 1.02$ pu, $U_j = 1$ pu, and $\delta_{ij} = 0.1$ rad, which gives the gradient,

$$\nabla_x P_{ij}^{loss}\left(\begin{bmatrix} 1.02 \\ 1.00 \\ 0.10 \end{bmatrix}\right) = 2g_{ij}\begin{bmatrix} 0.02500 \\ -0.01490 \\ 0.10183 \end{bmatrix}. \quad (10)$$

The sensitivity of losses to voltage magnitude has increased greatly, with the sensitivity of losses to the angle difference now only about 4 to 7 times larger. This suggests that inclusion of voltage magnitude effects into the loss formulation could result in nontrivial improvements in the model performance for conditions away from a flat voltage profile. □

Unfortunately, with the inclusion of voltage magnitudes, losses can no longer be expressed in a piecewise-linear form as is done when only angle difference is considered. In this situation, the formation of a set of linear inequalities becomes useful. As discussed in Section III, it is desirable to use a small number of constraints to capture the most important function characteristics, and to ensure tightness of the model by selecting linearization points from regions where the function exhibits convexity.

The (local) convexity/concavity of the loss function (5), in terms of bus voltage magnitudes and the angle difference, is given by the eigenvalues of the Hessian (8). If all the eigenvalues are positive then the function is convex in a region around the operating point. If there are both positive and negative eigenvalues then the function is a saddle, exhibiting convexity in some directions and concavity in others. This motivates the following theorem.

Theorem 1. *The Hessian matrix* (8) *of the line loss function* (5) *has exactly two positive eigenvalues over the region given by* $U_i > 0$, $U_j > 0$, $\delta_{ij} \in [-\frac{\pi}{2}, \frac{\pi}{2}]$.

Proof. The (scaled) Hessian matrix, $H = \frac{1}{2g_{ij}}\nabla_{xx}^2 P_{ij}^{loss}(x)$, can be expressed symbolically as,

$$H = \begin{bmatrix} a & b & c \\ b & d & e \\ c & e & f \end{bmatrix}. \quad (11)$$

This matrix is symmetric and may be decomposed into factors $H = LDL^\intercal$ where,

$$L = \begin{bmatrix} 1 & 0 & 0 \\ L_{21} & 1 & 0 \\ L_{31} & L_{32} & 1 \end{bmatrix}, \qquad D = \begin{bmatrix} D_1 & 0 & 0 \\ 0 & D_2 & 0 \\ 0 & 0 & D_3 \end{bmatrix}.$$

If the factorization exists, the signs of the diagonal elements of D will match the signs of the eigenvalues of H [18]. The elements of D can be expressed in terms of the entries in H as,

$$D_1 = a$$
$$D_2 = d - \frac{b^2}{a}$$
$$D_3 = f - \left(\frac{c^2}{a} + \frac{(ae - bc)^2}{a^2d - ab^2}\right).$$

Substituting for terms from (8) and simplifying gives,

$$D_1 = 1 \quad (12a)$$
$$D_2 = \sin^2(\delta_{ij}) \quad (12b)$$
$$D_3 = -(U_i^2 + U_j^2 + U_iU_j\cos(\delta_{ij})), \quad \text{for } \delta_{ij} \neq 0. \quad (12c)$$

When $\delta_{ij} \neq 0$, (12) provides a well-defined decomposition of H, with D_1 and D_2 both positive and D_3 negative. This implies that H has two positive eigenvalues and one negative eigenvalue. When $\delta_{ij} = 0$, D_3 is ill-defined due to a $\frac{0}{0}$ term and the decomposition does not exist. However, in this case substituting $\delta_{ij} = 0$ directly into (8) gives,

$$H = \begin{bmatrix} 1 & -1 & 0 \\ -1 & 1 & 0 \\ 0 & 0 & U_iU_j \end{bmatrix},$$

which has eigenvalues 0, 2 and $U_i U_j$. Since the voltage magnitudes are assumed to be strictly positive, the Hessian will have two positive eigenvalues and a single zero eigenvalue. □

The eigenvalues λ and eigenvectors v of the Hessian matrix $\nabla_{xx}^2 P_{ij}^{loss}(x)$ can be used to establish conditions which ensure the second-order term of the Taylor-series expansion (6) is positive,

$$\Delta x^\mathsf{T} \nabla_{xx}^2 P_{ij}^{loss}(x) \Delta x \geq 0. \tag{13}$$

Let Δx be expressed as a linear combination of the eigenvectors,

$$\Delta x = a v_1 + b v_2 + c v_3.$$

Then (13) becomes,

$$(a v_1 + b v_2 + c v_3)^\mathsf{T} \nabla_{xx}^2 P_{ij}^{loss}(x)(a v_1 + b v_2 + c v_3) \geq 0. \tag{14}$$

Since v_1, v_2, and v_3 are the eigenvectors of $\nabla_{xx}^2 P_{ij}^{loss}(x)$, this gives,

$$(a v_1 + b v_2 + c v_3)^\mathsf{T} (a\lambda_1 v_1 + b\lambda_2 v_2 + c\lambda_3 v_3) \geq 0. \tag{15}$$

Because $\nabla_{xx}^2 P_{ij}^{loss}(x)$ is symmetric, the eigenvectors can be expressed orthonormally so that $v_i^\mathsf{T} v_i = 1$ and $v_i^\mathsf{T} v_j = 0$ for $i \neq j \in \{1, 2, 3\}$. Accordingly, (15) becomes,

$$a^2 \lambda_1 + b^2 \lambda_2 + c^2 \lambda_3 \geq 0. \tag{16}$$

Since one of the eigenvalues is nonpositive while the other two are positive, equality in (16) describes an elliptic cone in the eigenbasis coordinates a, b, c. When the inequality is strictly greater than zero, it describes an elliptic hyperboloid. Any directions lying outside the cone will cause the second-order term in (6) to be positive. The centerline of the cone is given by the eigenvector associated with the negative eigenvalue. The minor and major axes of the elliptic cross-section of the cone are defined by the eigenvectors associated with the positive eigenvalues. The span of the two eigenvectors associated with the positive eigenvalues defines a plane which is perpendicular to the centerline of the cone. Figure 2 shows these surfaces for a typical voltage realization.

B. Loss model

The analysis of the Hessian motivates a loss model which (approximately) captures the variation in losses as voltages change from a given base voltage condition. This loss model comprises the loss linearization at the base voltage condition together with a set of loss linearizations formed by selecting neighboring voltage realizations. These neighboring points lie on the plane defined by the two eigenvectors associated with the positive eigenvalues. They are very likely to satisfy the convexity criterion necessary for a tight model as long as they remain sufficiently close to the original base operating point. This enables the model to capture the local convex nonlinearity of losses while largely eliminating the influence from the concave direction.

If prior knowledge of system behavior is available, the model can also be tuned to improve its accuracy for the likely changes. For instance, as shown in Fig. 2, one of the eigenvectors with a positive eigenvalue points primarily in the
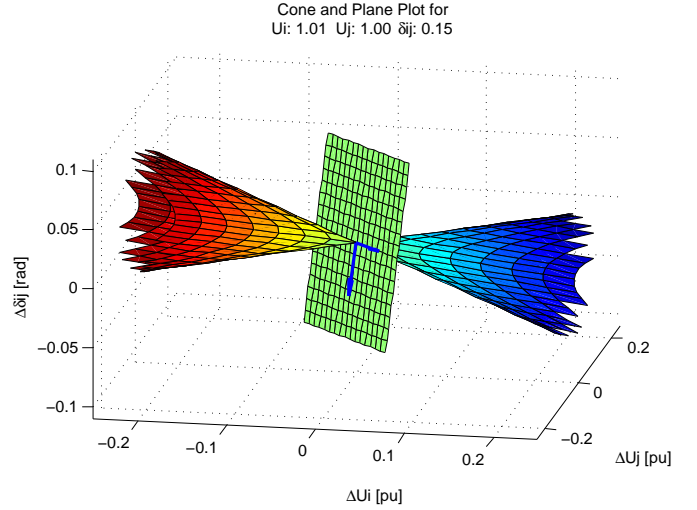

Fig. 2. Cone and plane defined by the eigen-decomposition of the loss function Hessian matrix. The second-order term of the Taylor-series expansion is positive for points outside the elliptic cone. The plane describes the span of the eigenvectors associated with the two positive eigenvalues.

direction of $\Delta \delta_{ij}$ with minimal changes to U_i and U_j. The other points primarily in the direction $+\Delta U_i$, $-\Delta U_j$ with minimal changes to δ_{ij}. If it is known that voltage magnitudes will not vary significantly, more linearization neighbors can be biased in the direction of the first eigenvector to better capture the nonlinearity in that direction.

V. TRENDS IN THE EIGENDECOMPOSITION OF LOSSES

When voltage conditions across the line change, the eigenvectors and eigenvalues of the Hessian matrix of the loss function will also change. For the greatest accuracy, the position of the neighboring linearization points relative to the base voltage condition should also be updated by finding the new eigenvectors of the Hessian. Doing so will ensure that the most significant nonlinearity of the function is captured by the loss model. However, if computational limits require more rapid implementation of loss model updates, the eigenvectors need not be recomputed for small changes in voltage conditions.

A. Consistency in eigenvector orientation

Over the range of typical power system voltages, U_i, $U_j \in [0.9, 1.1]$ pu and $|\delta_{ij}| \in [0, \pi/6]$ rad, the orientation of the eigenvectors of the loss Hessian remain relatively constant. Figure 3 shows the three eigenvectors over the set of voltages, U_i, $U_j \in \{0.9, 1, 1.1\}$, $|\delta_{ij}| \in \{0, \pi/60, \pi/30, \ldots, \pi/6\}$. The eigenvector v_3 associated with the larger positive eigenvalue is identified by black squares. It remains almost unchanged in the direction $[\Delta U_i \ \Delta U_j \ \Delta \delta_{ij}] = [-\frac{1}{\sqrt{2}} \ \frac{1}{\sqrt{2}} \ 0]$. As the angle difference across the line increases in magnitude, the other two eigenvectors rotate slightly around v_3. Changes in voltage magnitude have negligible effect on the orientation of the eigenvectors. When $|\delta_{ij}| \approx 0$, the eigenvector v_2 with the smaller positive eigenvalue, identified by blue circles, points in the general direction $[\Delta U_i \ \Delta U_j \ \Delta \delta_{ij}] = [0 \ 0 \ 1]$, and the eigenvector v_1 with the negative eigenvalue, indicated by
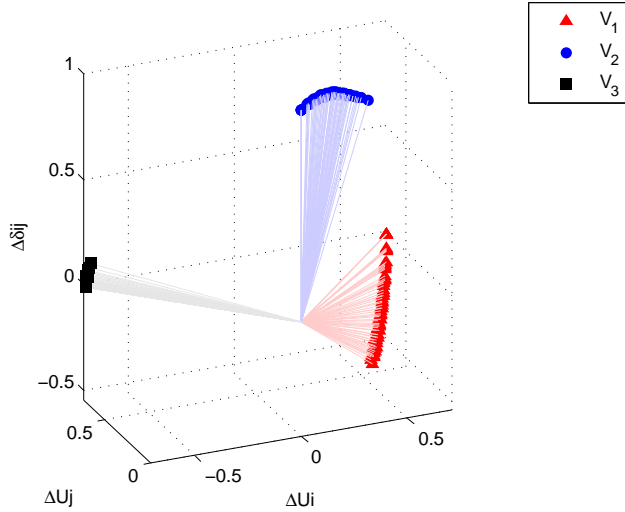
Fig. 3. Eigenvectors of the loss Hessian for typical network voltages, U_i, $U_j \in \{0.9, 1, 1.1\}$, $|\delta_{ij}| \in \{0, \pi/60, \pi/30, \ldots, \pi/6\}$. Eigenvectors are ordered by sorting the eigenvalues from negative to positive.

red triangles, points in the direction $[\Delta U_i \ \Delta U_j \ \Delta \delta_{ij}] = [\frac{1}{\sqrt{2}} \ \frac{1}{\sqrt{2}} \ 0]$.

Based on these observations, the eigenvectors of the loss Hessian may not need to be updated when changes in the angle difference across the line are less than 10 degrees. Using the previous eigenvectors to define the directions of the neighboring linearizations will still adequately capture the nonlinearity of the new loss condition and will save time in the computation of the updated loss model.

B. Eigenvalue magnitudes

Over typical operating voltages, the eigenvalues of the loss Hessian change in a predictable manner. Both positive eigenvalues are significantly larger in magnitude than the negative eigenvalue. Figure 4 shows the eigenvalues of the scaled loss Hessian, $\frac{1}{2g_{ij}} \nabla^2_{xx} P^{loss}_{ij}(x)$, over the set of voltages, U_i, $U_j \in \{0.9, 1, 1.1\}$, $|\delta_{ij}| \in \{0, \pi/60, \pi/30, \ldots, \pi/6\}$. The larger positive eigenvalue, λ_3 in Fig. 4, remains relatively constant over all typical voltage conditions. The smaller positive eigenvalue, λ_2, increases as voltage magnitudes increase while the negative eigenvalue, λ_1, remains mostly unchanged. When the angle difference across the line increases in magnitude, λ_1 decreases (becomes more negative) while λ_2 increases at almost the same rate. For small angle differences, the negative eigenvalue is approximately zero.

Although the proposed loss model does not include additional linearization neighbors in the direction of the eigenvector associated with the negative eigenvalue, the loss function exhibits very little nonlinearity in this direction. The negative eigenvalue, λ_1, is much smaller in magnitude than the two positive eigenvalues. This means that the linearization at the base voltage condition will sufficiently describe the behavior of the loss function in this direction and any overestimation of losses will be slight.
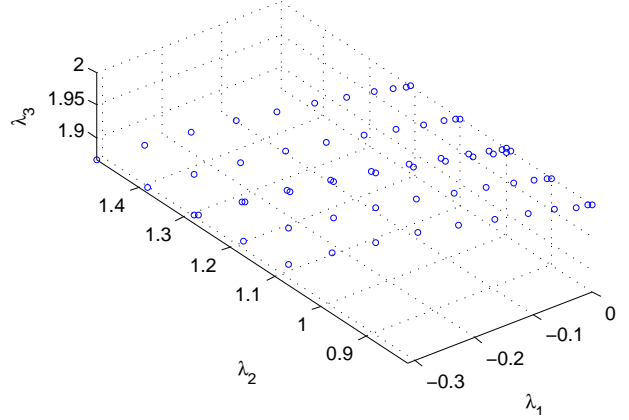

Fig. 4. Eigenvalues of the scaled loss Hessian, $\frac{1}{2g_{ij}} \nabla^2_{xx} P^{loss}_{ij}(x)$, for typical network voltages, U_i, $U_j \in \{0.9, 1, 1.1\}$, $|\delta_{ij}| \in \{0, \pi/60, \pi/30, \ldots, \pi/6\}$. Eigenvalues are ordered by sorting from negative to positive.

VI. APPLICATION TO LOWER DIMENSIONAL MODELS

A. Fixing one bus voltage magnitude

The model discussed in Section IV assumes that both the voltage magnitudes and the angle difference between them are allowed to vary. However, the presence of buses with fixed voltage magnitudes, such as generator buses, may mean that one or more of the voltage magnitudes in the line loss model remain constant. The effect of this modification is reflected in the eigenvalues of the Hessian in the resulting two-dimensional space.

Removing the row and column from (8) associated with a fixed voltage magnitude $U_{fix} \in \{U_i, U_j\}$ results in the Hessian matrix,

$$\nabla^2_{xx} P^{loss}_{ij}(x) = 2g_{ij} \begin{bmatrix} 1 & U_{fix} \sin(\delta_{ij}) \\ U_{fix} \sin(\delta_{ij}) & U_{free} U_{fix} \cos(\delta_{ij}) \end{bmatrix}, \tag{17}$$

where $x \equiv [U_{free} \ \delta_{ij}]^\intercal$. This matrix will always have at least one positive eigenvalue due to the '1' on the main diagonal and will be positive definite within the operating range $0.5 \leq U_i, U_j \leq 1.5$ pu, $|\delta_{ij}| \leq \frac{\pi}{6}$ rad. If the voltage magnitudes are closer to one, the angle difference criterion relaxes to about $\frac{\pi}{4}$ rad. The positive definite characteristic of the Hessian means that any direction can be used to establish neighboring linearizations for the line-loss relaxation.

B. Fixing both bus voltage magnitudes

When both bus voltage magnitudes are fixed and only the angle difference across the line is allowed to vary, the Hessian matrix reduces to a single term,

$$\nabla^2_{xx} P^{loss}_{ij}(\delta_{ij}) = 2g_{ij} U_i U_j \cos(\delta_{ij}). \tag{18}$$

This term is positive in the operating region $0 < U_i, U_j$ and $|\delta_{ij}| < \frac{\pi}{2}$ rad. The resulting model in this situation is very similar to a typical piecewise-linear approximation except that it provides a better loss estimate around the specified base voltage condition by utilizing the true voltage magnitudes instead of assuming they are fixed at 1 pu.

VII. Demonstration

A. Modelling process

The steps required to set up the proposed loss model for a single transmission line are outlined as follows:

1) Find the eigenvalues and eigenvectors of the Hessian matrix of the loss function, $\nabla_{xx}^2 P_{ij}^{loss}(x_0)$, for the base voltage condition.

2) Select neighboring voltage realizations, $x_1, \ldots, x_n$, within a relatively small ball on the plane spanned by the eigenvectors associated with the two positive eigenvalues of the Hessian matrix.

3) Define the linear inequality,

$$P_{ij}^{loss,app}(x) \geq P_{ij}^{loss}(x_k) + \nabla_x P_{ij}^{loss}(x_k)^{\mathsf{T}}(x - x_k),$$

for the loss equation at each point $x_k \in \{x_0, x_1, \ldots, x_n\}$ using (5) and (7). The complete loss model can then be expressed as,

$$P_{ij}^{loss,gen}(x) = \max \Big\{ 0,$$
$$\max_{k \in \{0,\ldots,n\}} \big\{ P_{ij}^{loss}(x_k) + \nabla_x P_{ij}^{loss}(x_k)^{\mathsf{T}}(x - x_k) \big\} \Big\},$$
$$(19)$$

where the outer 'max' ensures that the loss model cannot return a negative value. The superscript 'gen' identifies this as the generalized model, which will be referred to in later discussions as AC-GEN.

4) Confirm that each inequality is the binding constraint at its own linearization point, i.e. $P_{ij}^{loss,app}(x_k) = P_{ij}^{loss}(x_k)$ for each $k = 0, \ldots, n$. Discard any constraints which do not satisfy this criterion.

If the neighboring voltage realizations conditions are selected well by remaining relatively close to the base voltage condition, step 4) should rarely discard any constraints.

This process can be tuned to improve performance when specific voltage changes are likely or more significant. For instance, in networks where voltage magnitudes change little, linearization neighbors can be biased in the direction of the eigenvector which emphasizes changes in angle difference.

B. Case-study description

The performance of the proposed approach (AC-GEN) is compared against two common linear loss models. The first is a simple first-order Taylor-series expansion of the line loss equation (5) in terms of voltage magnitudes and angle difference,

$$P_{ij}^{loss,lin}(x) = P_{ij}^{loss}(x_0) + \nabla_x P_{ij}^{loss}(x_0)^{\mathsf{T}}(x - x_0), \quad (20)$$

which will be referred to as AC-LIN. The second is a piecewise-linear approximation of the squared angle difference which ignores voltage magnitudes (DC-PWL) [13]. Each loss modelling technique is employed to approximate the line loss equation (5) for every line in a network.

Both the AC-GEN and DC-PWL models require various input parameters. DC-PWL requires the maximum possible angle difference across the line and the number of segments
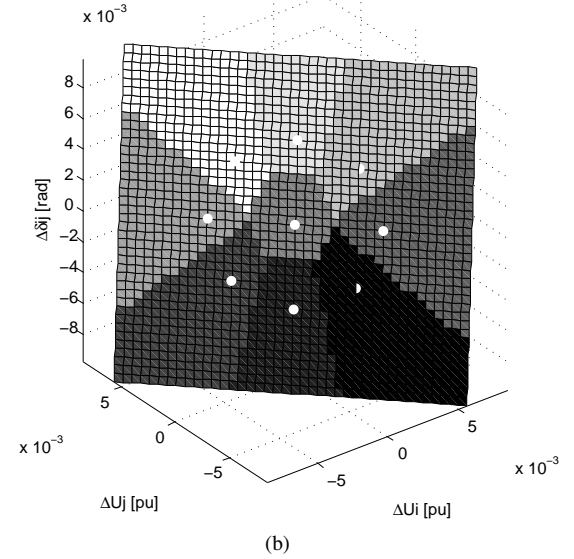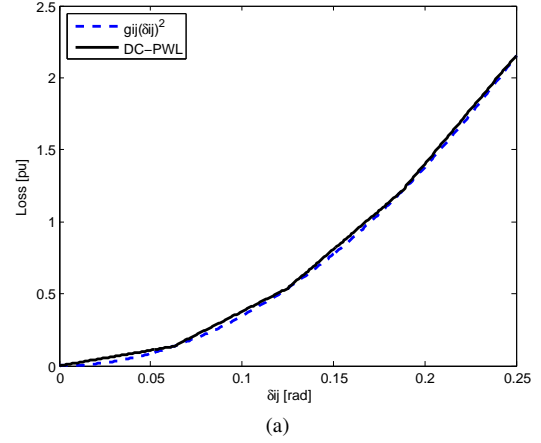

Fig. 5. Sample representations for DC-PWL and AC-GEN. (a) DC-PWL only considers variation in angle difference. (b) AC-GEN behavior on the plane spanned by the eigenvectors associated with the positive eigenvalues of the Hessian. White dots indicate linearization points. Shading indicates the regions where each linear inequality is binding.

to use in the piecewise linear approximation. For this analysis, the maximum angle was set to 2.5 times the angle at the line rating, $\delta_{ij}^{max} = 2.5 X_{ij} P_{ij}^{lim}$ using a dc power flow approximation. This range was broken into 25 segments. AC-GEN requires the distance from the base voltage condition, x_0, to the neighboring voltage realizations, $x_1, \ldots, x_n$. For this analysis, eight evenly spaced neighboring realizations were selected from the edge of a circle on the plane spanned by the two eigenvectors associated with positive eigenvalues. The radius of this circle was chosen to be 0.005 pu. Figure 5 exemplifies how each of these modelling approaches sectionalizes the space of voltage variables, $[U_i \ U_j \ \delta_{ij}]$, to approximate the nonlinear losses.

To demonstrate the operational characteristics on a realistically large network, the MATPOWER [19] test case based on the 2383-bus Polish grid for the 1999-2000 winter peak was used for the discussions in this section. This test network provides a wide variety of realistic voltage and impedance characteristics. Since losses are only affected by

series conductance, g_{ij}, the R/X ratios of the lines do not directly affect the various loss models. However, different impedance characteristics cause the voltages across lines to vary in different ways, providing a variety of test conditions for the three loss models.

Testing was undertaken for 25 different scenarios. Five random base-case power flow scenarios were generated and then five random demand deviations were established for each base-case. For each of the 25 scenarios, a power flow captured the true line losses and the voltage deviations from the corresponding base-case. The voltage deviations were applied to each loss model to calculate its estimated losses. The models for AC-GEN and AC-LIN require a starting voltage condition and were updated for each base-case scenario. The DC-PWL model does not depend upon initial voltages so was generated once at the start of testing. Each base-case scenario was created by randomly perturbing active and reactive power loads. Active power loads were uniformly distributed over the range $\pm 50\%$ of their values given in the MATPOWER case, while reactive power loads were uniformly distributed over the range $\pm 30\%$ of their MATPOWER values. The deviation cases were likewise created by randomly perturbing active and reactive power loads, in this case over the ranges $\pm 50\%$ and $\pm 30\%$, respectively, of their values in the corresponding base-case scenario.

C. Accuracy comparison

The errors between the actual line losses and the losses predicted by each model, for all lines in the Polish network across all 25 tests, giving a total of $L = 2896 \times 25 = 72,400$ cases, are summarized in Fig. 6 and Table I. The results of Fig. 6a show the loss prediction error, $\mathrm{Err}_\ell = \mathrm{est}_\ell - \mathrm{act}_\ell$, in per unit, while Fig. 6b provides additional perspective by normalizing these errors, $\%\mathrm{Err}_\ell = 100 \times (\mathrm{est}_\ell - \mathrm{act}_\ell)/\mathrm{act}_\ell$. Normalized errors were ignored for loss values less than 1×10^{-4} pu. The AC-GEN model (19) and the DC-PWL model [13] are structured such that they do not allow negative losses. Consequently, their normalized errors cannot fall below -100%. This limit is evident in Fig. 6b. In contrast, losses computed by the AC-LIN model (20) are directly dependent upon voltage values and therefore may go negative. Fig. 6b also highlights the tendency for AC-GEN and AC-LIN to underestimate the loss function since it is convex in most directions and only weakly concave otherwise.

As expected, the AC-GEN and AC-LIN methods are both more accurate than the DC-PWL method for small changes in voltage conditions, as shown in Fig. 6a for voltage changes between 0 and 0.02 pu. Both AC-GEN and AC-LIN start from a tight approximation of losses due to the linearization around the base-case whereas DC-PWL has no mechanism for using base-case information. For voltage changes beyond 0.005 pu, AC-GEN improves upon AC-LIN due to the additional linearizations at neighboring voltage realizations, but both methods show quadratic growth in their error for large voltage deviations. This is due to their underlying local linearization structure. In contrast, the broader nonlinear characteristic of the DC-PWL method helps to suppress some of this behavior.
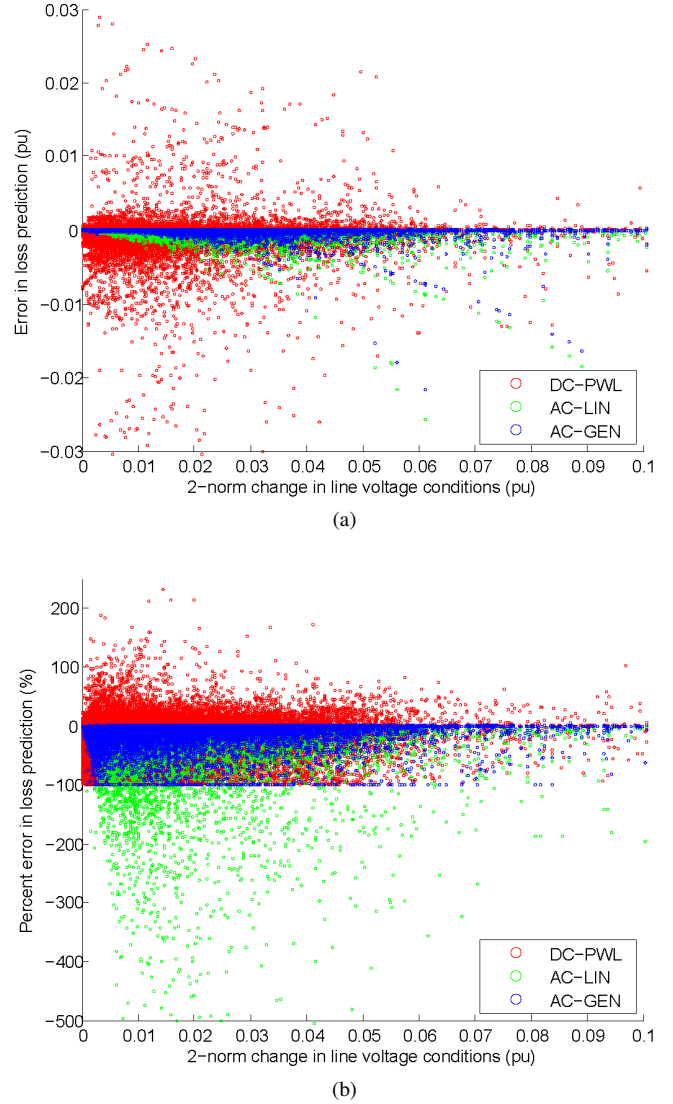

(a)

(b)

Fig. 6. Errors between actual and estimated line losses for 25 tests on the Polish 2383-bus network. The x-axis position is determined using $\sqrt{\Delta U_i^2 + \Delta U_j^2 + \Delta \delta_{ij}^2}$. (a) Error in pu, $\mathrm{Err} = \mathrm{est} - \mathrm{act}$. (b) Error in percent, $\%\mathrm{Err} = 100 \times (\mathrm{est} - \mathrm{act})/\mathrm{act}$. Percent error for losses less than 1×10^{-4} pu is ignored.

TABLE I
AVERAGE LOSS ERROR OVER 25 TESTS ON THE POLISH 2383-BUS NETWORK.

Method	$\frac{1}{L}\sum_{\ell=1}^{L} \mathrm{Err}_\ell$, pu	$\frac{1}{L}\sum_{\ell=1}^{L} |\mathrm{Err}_\ell|$, pu	$\frac{1}{L}\sum_{\ell=1}^{L} |\%\mathrm{Err}_\ell|$, %
AC-GEN	-4.6×10^{-5}	4.6×10^{-5}	5.88
AC-LIN	-1.0×10^{-4}	1.0×10^{-4}	13.46
DC-PWL	-2.6×10^{-4}	4.4×10^{-4}	24.21

The summary in Table I assists in clarifying the overall performance of each method. The error summations given in the first column take into account the sign of the error and therefore provide an indication of the total system-wide error (with positive and negative errors partially cancelling). The other columns consider the absolute value of the error, giving
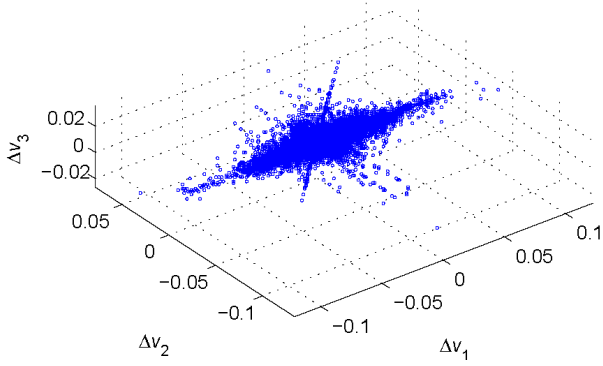
Fig. 7. Perturbations in line voltages expressed in eigenbasis coordinates for all lines of the 25 tests on the Polish 2383-bus network. Eigenvectors of the Hessian for each line are ordered by sorting the eigenvalues from negative to positive.
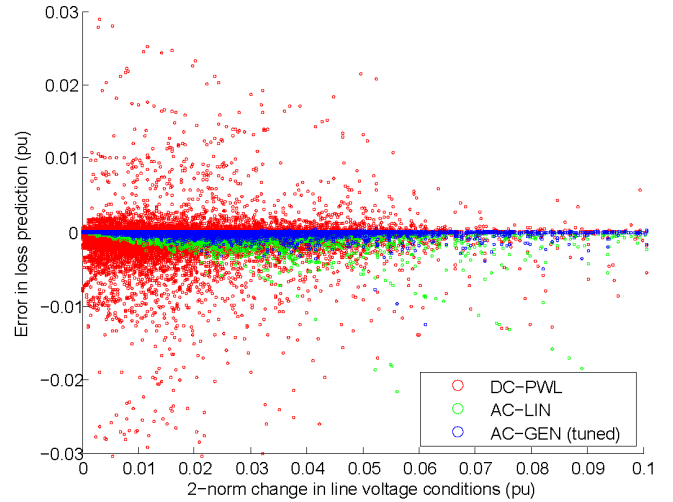

Fig. 8. Errors between actual and estimated line losses for 25 tests on the Polish 2383-bus network. AC-GEN has been tuned for each line. The x-axis position is determined using $\sqrt{\Delta U_i^2 + \Delta U_j^2 + \Delta \delta_{ij}^2}$. The y-axis shows error in pu, $\mathrm{Err} = \mathrm{est} - \mathrm{act}$.

a better indication of the overall trend in line-by-line errors. In that sense, the right-most column is most relevant, providing a comparison of the average absolute value of the normalized errors. The AC-GEN method is more than twice as accurate as the AC-LIN method and more than four times as accurate as the DC-PWL method. Even though the 25 test cases exhibit significant variation in active and reactive power loads, and hence in network voltages, the AC-GEN loss model generally provides very good accuracy.

D. Tuning the AC-GEN model

The results shown in Fig. 6 and Table I indicate that even an untuned application of the proposed loss model can result in appreciable improvements in accuracy compared to existing methods. In those tests, the distance to the linearization neighbors was the same for every line. However, voltages change much more noticeably on some lines than others and the AC-GEN model can easily be tuned to capture this effect. Additionally, voltage changes tend to be much larger in the direction of the eigenvector with the smaller positive eigenvalue than in the direction of the eigenvector with the larger positive eigenvalue. This trend can also be used to better model the unique loss characteristics of each line.

The perturbations in voltages for each of the 25 tests can be transformed into the eigenbasis coordinates of the loss Hessian for each line, $[\Delta U_i \ \Delta U_j \ \Delta \delta_{ij}]^\mathsf{T} = \Delta v_1 \times v_1 + \Delta v_2 \times v_2 + \Delta v_3 \times v_3$ where Δv_i is the scalar coordinate associated with eigenvector v_i. Figure 7 shows this eigenbasis representation. It is apparent that voltage changes lie primarily in the direction of v_1, the eigenvector with a negative eigenvalue. Modest changes occur in the direction of v_2, the eigenvector with the smaller positive eigenvalue, and only limited changes occur in the direction of v_3, the eigenvector with the larger positive eigenvalue. Although AC-GEN avoids linearization neighbors in the direction of v_1, the loss function is approximately linear in this direction and the base linearization sufficiently describes these changes.

Analyzing the results of Fig. 7 reveals that voltage changes in the direction of v_2 are approximately five times larger than those in the v_3 direction. To better capture this pattern, the

circle of white dots shown in Fig. 5b was flattened into an ellipse whose axis in the direction of v_2 is five times the length of the axis in the direction of v_3. Additionally, two extra linearization neighbors were added in the direction of v_2 at twice the distance from the base condition. These helped capture even larger voltage changes in this direction.

The majority of voltage changes in Fig. 7 are very close to the origin. However, some lines tend to experience much larger changes in voltage than others. Such prior knowledge can be used to establish, on a line-by-line basis, the length of the minor axis of the ellipse that describes the locations of the linearization neighbors.

The tuned AC-GEN model was tested on the same data as previously. The results are shown in Fig. 8. Comparing with Fig. 6a, it can be seen that tuning has resulted in additional improvements in overall accuracy and has eliminated the larger errors. The mean absolute error in the loss prediction, $\frac{1}{L} \sum_{\ell=1}^{L} |\mathrm{Err}_\ell|$, is reduced to 3.0×10^{-5} pu or 2.55%. This type of tuning could easily be implemented in practice by using readily available historical data and performing more sophisticated data analysis.

E. Computational comparison

In addition to considering the model accuracy, it is important to evaluate the influence of the loss model on the speed of optimization and control applications. To test this characteristic, each of the three models was applied within a simple quadratic program (QP) which sought to drive voltage magnitudes and angles towards specified values while also minimizing total network losses.[1] This QP was run for each of the 25 test cases. The only constraints in each program were the loss models relating line losses to network voltages and a single summation

---

[1] The QP was not meant to address any real problem, but rather provide a means of establishing the relative computational costs of the three loss modelling formulations.

TABLE II
QP TEST RESULTS FOR VARIOUS LOSS MODELS.

Method	EQs	INEQs	VARs	Build Time [μs/line]	SOLN Time [s]
AC-GEN	1	26064	7663	167.	1.14
AC-LIN	2897	0	7663	3.14	0.02
DC-PWL	8689	0	85855	12.7	0.78

of all line losses into total losses. Testing was performed on an HP ProBook 6470b with a 2.90 GHz Intel® i7 processor and 8 GB of RAM. The QP was formulated in MATLAB® and solved in Gurobi [20].

A summary of the QP constraint sets and the time required to build the loss model and solve each QP for each of the 25 test cases is presented in Table II. The AC-LIN method has the smallest set of constraints and can be built and solved significantly faster than both the untuned AC-GEN and DC-PWL methods. The untuned AC-GEN method requires the most time to build and solve and takes about 46% longer to solve than the DC-PWL method. If the eigenvectors are not updated when building the AC-GEN model, the build time can be reduced by around 30%.

F. Discussion of results

From the results of the case-study tests, it is apparent that trade-offs exist for each of the three methods. Subject to the formulation requirements discussed in Section II, AC-GEN offers the greatest accuracy in predicting line losses. However, this improvement in accuracy requires an increase in the time to build and solve the model. Alternatively, if memory and time constraints are of primary concern, a simple linear model may provide acceptable accuracy depending on the application.

Several challenges may arise from incorporating a line-loss model into optimal power flow problems for both operational cost minimization and expansion planning. When negative prices are possible, any relaxation method (e.g. AC-GEN or DC-PWL) may cease to provide a tight solution as fictitious losses can reduce the overall cost [21], [22]. In this situation, a heuristic is necessary to remove the fictitious losses. For the AC-GEN method, the simplest solution is to use the AC-LIN model on any line connected to a bus with negative price. Also, [14] points out that the types of loss models discussed here can slow convergence by inducing oscillations as they approach a solution. Unfortunately, the nonconvexity of the loss function when voltage magnitude variations are considered prohibits the extension of the method in [14] where successive "cutting planes" are added. However, to limit oscillations in the AC-GEN method, the distance to the linearization neighbors can be reduced as the solution is approached.

Another challenge with loss models which require updates as operating conditions change (e.g. AC-GEN and AC-LIN) is that these steps require additional computation. For the AC-LIN method, these costs are very small but AC-GEN may require some consideration depending on the application. For

best results, AC-GEN should be updated whenever network voltages change. However, if these changes are small and remain within the region bounded by the linearization neighbors, it may be acceptable to retain the previous model. Ultimately, the design needs of the specific application will determine whether accuracy or speed is more important.

VIII. CONCLUSION

This paper proposes a new relaxed loss formulation for computing losses on a transmission line when voltages are expressed in polar coordinates and voltage magnitudes may vary. A systematic approach is developed to build a set of linear inequalities which underbound the true losses. In a region around the base voltage condition, the resulting loss model is more accurate than existing linear and piecewise-linear formulations. The model can be tuned to capture voltage behavior on specific lines and offers the potential to achieve improved performance in applications which require accurate loss calculation on a line-by-line basis.

The application environments which are likely to benefit the most from the AC-GEN formulation are those which model losses on a small number of lines, require a linear constraint formulation, but also require good accuracy. Examples include controllers that thermally model lines near their flow limit [23]. In situations where line losses are required to predict thermal behavior, small improvements in the line loss accuracy can result in amplified improvements in the temperature prediction.

REFERENCES

[1] E. E. George, "Intrasystem transmission losses," *AIEE Transactions*, vol. 62, no. 3, pp. 153-158, Mar. 1943.
[2] J. B. Ward *et al.*, "Total and incremental losses in power transmission networks," *AIEE Transactions*, vol. 69, no. 1, pp. 626-632, Jan. 1950.
[3] L. K. Kirchmayer and G. W. Stagg, "Analysis of total and incremental losses in transmission systems," *AIEE Transactions*, vol. 70, no. 2, pp. 1197-1205, Jul. 1951.
[4] W. R. Brownlee, "Co-ordination of incremental fuel costs and incremental transmission losses by functions of voltage phase angles," *AIEE Trans. Power App. Syst., Part III*, vol. 73, no. 1, pp. 529-533, Jan. 1954.
[5] J. E. Van Ness, "A note on incremental loss computation," *AIEE Trans. Power App. Syst., Part III*, vol. 81, no. 3, pp. 735-737, Apr. 1962.
[6] J. R. Tudor and W. A. Lewis, "Transmission losses and economy loading by the use of admittance constants," *IEEE Trans. Power App. Syst.*, vol. 82, no. 68, pp. 676-683, Oct. 1963.
[7] S. de la Torre and F. D. Galiana, "On the convexity of the system loss function," *IEEE Trans. Power Syst.*, vol. 20, no. 4, pp. 2061-2069, Nov. 2005.
[8] E. F. Hill and W. D. Stevenson, "A new method of determining loss coefficients," *IEEE Trans. Power App. Syst.*, vol. 87, no. 7, pp. 1548-1553, Jul. 1968.
[9] F. D. Galiana and M. Banakar, "Approximation formulae for dependent load flow variables," *IEEE Trans. Power App. Syst.*, vol. 100, no. 3, pp. 1128-1137, Mar. 1981.
[10] G. L. Torres and V. H. Quintana, "An interior-point method for non-linear optimal power flow using voltage rectangular coordinates," *IEEE Trans. Power Syst.*, vol. 13, no. 4, pp. 1211-1218, Nov. 1998.
[11] R. A. Jabr, "Modeling network losses using quadratic cones," *IEEE Trans. Power Syst.*, vol. 20, no. 1, pp. 505-506, Feb. 2005.
[12] H. Zhong *et al.*, "Dynamic economic dispatch considering transmission losses using quadratically constrained quadratic program method," *IEEE Trans. Power Syst.*, vol. 28, no. 3, pp. 2232-2241, Aug. 2013.
[13] A. L. Motto *et al.*, "Network-constrained multiperiod auction for a pool-based electricity market," *IEEE Trans. Power Syst.*, vol. 17, no. 3, pp. 646-653, Aug. 2002.
[14] T. N. dos Santos and A. L. Diniz, "A dynamic piecewise linear model for dc transmission losses in optimal scheduling problems," *IEEE Trans. Power Syst.*, vol. 26, no. 2, pp. 508-519, May 2011.

[15] C. Coffrin, P. Van Hentenryck, and R. Bent, "Approximating line losses and apparent power in AC power flow linearizations," in *2012 IEEE Power and Energy Society General Meeting*, San Diego, CA, 2012.

[16] H. M. Ayres *et al.*, "Evaluation of the impact of distributed generation on power losses by using a sensitivity-based method," in *Proc. 2009 IEEE PES General Meeting*, pp. 1-6.

[17] H. M. Ayres, D. Salles, and W. Freitas, "A practical second-order based method for power losses estimation in distribution systems with distributed generation," *IEEE Trans. Power Syst.*, vol. 29, no. 2, pp. 666-674, Mar. 2014.

[18] G. Strang, "Semidefinite and indefinite matrices," in *Linear Algebra and its Applications*, 3rd ed. San Diego, CA: Harcourt Brace Jovanovich, 1988, ch. 6, sec. 3, pp. 341.

[19] R. D. Zimmerman, C. E. Murillo-Sánchez, and R. J. Thomas, "MAT-POWER: steady-state operations, planning and analysis tools for power systems research and education," *IEEE Trans. Power Syst.*, vol. 26, no. 1, pp. 12-19, Feb. 2011.

[20] *Gurobi Optimizer Reference Manual*, Version 6.5, Gurobi Optimization, Inc., 2015.

[21] O. W. Akinbode and K. W. Hedman, "Fictitious losses in the DCOPF with a piecewise linear approximation of losses," in *2013 IEEE Power & Energy Society General Meeting*, Vancouver, BC, 2013, pp. 1-5.

[22] H. Zhang *et al.*, "An improved network model for transmission expansion planning considering reactive power and network losses," *IEEE Trans. Power Syst.*, vol. 28, no. 3, pp. 3471-3479, Aug. 2013.

[23] M. R. Almassalkhi and I. A. Hiskens, "Model-predicitive cascade mitigation in electric power systems with storage and renewables – part I: theory and implementation," *IEEE Trans. Power Syst.*, vol. 30, no. 1, pp. 67-77, Jan. 2015.

Jonathon A. Martin (S'13) received the B.S. degree in engineering from Messiah College, Mechanicsburg, PA, USA, in 2012 and is currently pursuing his Ph.D. degree in Electrical Engineering: Systems at the University of Michigan, Ann Arbor, MI, USA. His research interests include power systems analysis and control, optimization, and integration of renewable energy sources.

Ian A. Hiskens (F'06) is the Vennema Professor of Engineering in the Department of Electrical Engineering and Computer Science, University of Michigan, Ann Arbor. He has held prior appointments in the Queensland electricity supply industry, and various universities in Australia and the United States. His research interests lie at the intersection of power system analysis and systems theory, with recent activity focused largely on integration of renewable generation and controllable loads. Dr. Hiskens is actively involved in various IEEE societies, and was VP-Finance of the IEEE Systems Council. He is a Fellow of IEEE, a Fellow of Engineers Australia and a Chartered Professional Engineer in Australia.